



The Potential Role of Intensity-Modulated Proton Therapy in Hepatic Carcinoma in Mitigating the Risk of Dose De-Escalation

Technology in Cancer Research & Treatment
 Volume 19: 1-10
 © The Author(s) 2020
 Article reuse guidelines:
sagepub.com/journals-permissions
 DOI: 10.1177/1533033820980412
journals.sagepub.com/home/tct


Luca Cozzi, PhD^{1,2} , Tiziana Comito, MD¹, Mauro Loi, MD¹, Antonella Fogliata, MSc¹, Ciro Franzese, MD^{1,2}, Davide Franceschini, MD¹, Elena Clerici, MD¹, Giacomo Reggiori, MSc¹, Stefano Tomatis, MSc¹, and Marta Scorsetti, MD^{1,2}

Abstract

Purpose: To investigate the role of intensity-modulated proton therapy (IMPT) for hepatocellular carcinoma (HCC) patients to be treated with stereotactic body radiation therapy (SBRT) in a risk-adapted dose prescription regimen. **Methods:** A cohort of 30 patients was retrospectively selected as “at-risk” of dose de-escalation due to the proximity of the target volumes to dose-limiting healthy structures. IMPT plans were compared to volumetric modulated arc therapy (VMAT) RapidArc (RA) plans. The maximum dose prescription foreseen was 75 Gy in 3 fractions. The dosimetric analysis was performed on several quantitative metrics on the target volumes and organs at risk to identify the relative improvement of IMPT over VMAT and to determine if IMPT could mitigate the need of dose reduction and quantify the consequent potential patient accrual rate for protons. **Results:** IMPT and VMAT plans resulted in equivalent target dose distributions: both could ensure the required coverage for CTV and PTV. Systematic and significant improvements were observed with IMPT for all organs at risk and metrics. An average gain of 9.0 ± 11.6 , 8.5 ± 7.7 , 5.9 ± 7.1 , 4.2 ± 6.4 , 8.9 ± 7.1 , 6.7 ± 7.5 Gy was found in the near-to-maximum doses for the ribs, chest wall, heart, duodenum, stomach and bowel bag respectively. Twenty patients violated one or more binding constraints with RA, while only 2 with IMPT. For all these patients, some dose de-intensification would have been required to respect the constraints. For photons, the maximum allowed dose ranged from 15.0 to 20.63 Gy per fraction while for the 2 proton cases it would have been 18.75 or 20.63 Gy. **Conclusion:** The results of this in-silico planning study suggests that IMPT might result in advantages compared to photon-based VMAT for HCC patients to be treated with ablative SBRT. In particular, the dosimetric characteristics of protons may avoid the need for dose de-escalation in a risk-adapted prescription regimen for those patients with lesions located in proximity of dose-limiting healthy structures. Depending on the selection thresholds, the number of patients eligible for treatment at the full dose can be significantly increased with protons.

Keywords

intensity-modulated proton therapy, VMAT, RapidArc, liver cancer, stereotactic ablative radiation therapy

Received: June 29, 2020; Revised: October 05, 2020; Accepted: October 29, 2020.

Introduction

Stereotactic body radiotherapy (SBRT) demonstrated a relevant role in the management of hepatocellular carcinoma (HCC), one of the most common primary liver tumors.¹⁻⁴

The feasibility of SBRT was investigated by several groups. Wang et al⁵ reported about 20 patients treated with moderate hypofractionation and the use of volumetric modulated arc therapy (VMAT) showing its feasibility. The use of SBRT with

¹ Radiotherapy and Radiosurgery Department, Humanitas Clinical and Research Center, IRCSS, Milan-Rozzano, Italy

² Department of Biomedical Sciences, Humanitas University, Milan-Rozzano, Italy

Corresponding Author:

Luca Cozzi, Radiotherapy and Radiosurgery Department, Humanitas Clinical and Research Center, IRCSS, Via Manzoni 56, 20089—Milan-Rozzano, Italy.
 Email: luca.cozzi@humanitas.it



ablative intent for the treatment of HCC was reported by [anonymized]⁶ for a regimen of 3 fractions of 25 Gy each. The study included 43 patients treated with a risk-adapted scheme with 64% local control (LC) at 2 years and median overall survival (OS) of 18 months (45% survival at 2 years). The routine clinical practice on this subset of patients was based on this study in our institute. This aggressive fractionation scheme might not be absolutely necessary, at least for patients with targets near to normal tissues as demonstrated, e.g. by Duran-Labruine et al⁷ or Yoon et al⁸ with 45 Gy in 3 fractions, by Su et al⁹ with 42-48 Gy in 3 fractions, all with a biological equivalent dose (BED) greater than 100 Gy.

The evidence of the role of proton beam therapy (PBT) in HCC is increasing, as shown in Yeung's review study.¹⁰ Proton therapy may offer improved control rates with reduced toxicity levels due to its dosimetric features. In this perspective, the consensus report from the liver proton therapy conference held in Miami in 2018¹¹ analyzed the optimal utilization of PBT, concluding that it should be preferred when a suboptimal therapeutic ratio would be expected from photon therapy.

Hasan et al¹² analyzed the effects of dose escalation in a propensity-matched study from cancer registry and showed an increased survival for patients treated with protons compared to photon-based SBRT. Hsu et al¹³ reviewed the use of charged particle therapy (proton or ions) and confirmed the better LC and OS rates compared to photon beam therapy. Chada et al¹⁴ reported positive outcome results for localized unresectable HCC patients treated with moderate hypofractionation regimens. Sanford et al¹⁵ demonstrated that proton therapy was associated with improved survival and decreased risk of radiation-induced liver disease.

SBRT endeavors to respect the dose-volume constraints on organs at risk (OAR) in the proximity of the target in HCC patients. Kim et al¹⁶ reviewed a cohort of 243 patients who received a risk-adapted moderate SBRT proton treatment and concluded that protons have the potential to play a positive role across all stages of HCC. Mondlane et al¹⁷ performed a planning study on 10 patients previously treated with SBRT and compared the original photon plan to the intensity-modulated proton therapy (IMPT). The study demonstrated a significant decrease of the mean doses to the relevant organs at risk and the non-targeted part of the liver while maintaining similar target coverage. Gandhi et al¹⁸ simulated spherical tumors from 1 to 6 cm in diameter and located in 4 locations in the liver (dome, caudal, left medial and central). A decision model to predict the optimal modality was developed and validated on 10 real patients. The authors concluded that protons should be considered as preferable for the dome and central lesions greater than 3 cm in diameter. Protons were also recommended for any lesion greater than 5 cm if the photon plans would fail in achieving the thresholds for either target coverage or mean dose to the non-targeted liver.

In an earlier study, we investigated the role of IMPT for ablative SBRT and showed the feasibility of the method, also applying robust optimization (RO) in a cohort of 20 patients with advanced HCC and planned for 60 Gy in 3 fractions.¹⁹

The aim of the present study, in line with the consensus report,¹¹ was to investigate the role of IMPT compared to VMAT in mitigating the need for dose de-escalation in a risk-adapted prescription scheme starting from a more aggressive regimen of 3 fractions of 25 Gy each as in.⁶ It is clear that, with a gentler regimen (e.g 45 Gy) fewer patients might be exposed to the risk of dose de-escalation. This limitation, acknowledged as an a-priori fact, should not invalidate the scope of the investigation which is the appraisal of the potential role of IMPT. A cohort of potentially challenging patients was retrospectively chosen from the clinical database and re-planned for proton therapy, which was subsequently compared to photon plans.

Materials and Methods

Patient Selection, Contouring and Dose Prescription

A group of 30 patients was selected for this retrospective in-silico planning study (with notified prior approval from the ethics committee). All patients were unsuitable for other loco-regional therapies and were previously treated with stereotactic ablative radiation therapy, as described in.⁶ All patients signed informed consent to have data from their medical records used for research purpose. Patients were selected if one or more dose-volume planning aim with respect to the OARs resulted challenging or even unmet with the full dose prescription due to the position of the lesion.

All patients were scanned for imaging and treated under abdominal compression (AC) conditions. This was realized by means of thermoplastic body masks which included Styrofoam blocks to minimize the respiratory organ motion. The gross tumor volume (GTV) was defined on contrast-enhanced time-resolved planning computed tomography (4D-CT) co-registered with magnetic resonance images (MRI) to better identify the lesions. The clinical target volume (CTV) corresponded to the GTV. The planning target volume (PTV) was generated from the CTV by adding an overall isotropic margin of 4-6 mm in all directions.

The organs at risk (OAR) considered for the study were: the spinal cord, the kidneys, the stomach, the duodenum, the bowel bag, the heart, the ribs, the chest wall and the healthy liver (defined as the whole liver minus the PTV). Central hepatobiliary structures (CHB), not considered in clinical practice, were retrospectively added for the study. These were defined with an isotropic expansion of 15 mm from the portal vein as described by Toesca et al.²⁰⁻²²

The dose prescription was of 75 Gy in 3 fractions of 25 Gy normalized to the mean dose to the clinical target volume. The prescribed dose could be reduced according to an adaptive risk scheme if any dose-volume objective for the OARs would have been violated. The possible reduced dose levels were 22.50, 20.63, 18.75, 16.00, 15.00 Gy for 3 fractions.

The plan objective was to cover at least 98% of the CTV with 98% ($D_{98\%} \geq 98\%$) of the prescribed dose and for the PTV to cover 95% of the volume with the 95% isodose

Table 1. Summary of the Quantitative Analysis of the Dose-Volume Histograms for the Main Structures Over the Entire Cohort of Patients for the RapidArc Based Photon Plans and the Intensity-Modulated Proton Plans.

Structure	Objective	IMPT	RA	Δ	p
CTV					
D _{mean} [Gy]	=75	75.0 ± 0.0	75.0 ± 0.0	-	-
D98% [Gy]	≥73.5 (98%)	73.7 ± 0.6 [72.9;74.5]	73.8 ± 0.5 [72.7;74.5]	-0.1 ± 0.6 [-1.2;1.7]	ns
D1% [Gy]	-	77.1 ± 1.1 [75.7;79.5]	76.5 ± 0.5 [75.6;77.6]	0.6 ± 1.1 [-1.7;3.3]	ns
HI [%]	<5	3.0 ± 1.2 [1.4;5.6]	2.6 ± 1.1 [1.0;5.2]	0.4 ± 1.4 [-3.4;3.3]	ns
PTV					
D _{mean} [Gy]	=75	74.8 ± 0.4 [74.1;75.4]	74.5 ± 0.5 [72.9;75.5]	0.3 ± 0.4 [-0.5;1.4]	ns
D95% [Gy]	≥71.2 (95%)	71.5 ± 2.4 [67.8;74.5]	71.3 ± 1.7 [67.1;73.4]	0.2 ± 1.9 [-3.7;3.6]	ns
D1% [Gy]	-	78.4 ± 1.3 [76.4;81.7]	77.1 ± 0.4 [76.5;78.3]	1.4 ± 1.4 [-0.6;4.4]	0.003
Liver-PTV					
D _{mean} [Gy]	≤15	6.1 ± 2.8 [2.3;14.0]	11.1 ± 4.4 [3.7;19.0]	-4.9 ± 3.2 [-11.5;0.7]	<0.001
V<15Gy [cm ³]	≥700	1148.8 ± 404.2 [705.4;2238.6]	988.2 ± 397.6 [473.1;2103.1]	155.2 ± 167.1 [-105.1;758.3]	0.001
Central hepatobiliary structures (CHB)					
D _{mean} [Gy]	≤16.5	12.2 ± 15.3 [0.0;60.5]	17.9 ± 16.2 [0.6; -63.6]	-5.7 ± 6.0 [-23.5;3.8]	<0.001
V _{18.5Gy} [cm ³]	≤45	26.1 ± 29.1 [0.0;113.0]	38.9 ± 36.9 [0.0;123.7]	-12.8 ± 19.3 [-65.5;25.1]	<0.001
V _{22.5Gy} [cm ³]	≤37	23.4 ± 27.5 [0.0;113.0]	32.8 ± 34.2 [0.0;122.6]	-9.5 ± 14.6 [-48.3;21.1]	<0.001
Ribs					
D _{2cm3} [Gy]	≤30	23.8 ± 12.2 [0.0;70.6]	32.7 ± 16.7 [1.1;72.6]	-9.0 ± 11.6 [-39.5;6.6]	0.001
Chest wall					
D _{30cm3} [cm ³]	≤30	13.4 ± 9.8 [0.0;29.7]	21.5-11.2 [0.2;46.6]	-8.5 ± 7.7 [-26.9; -0.2]	0.03
Heart					
D _{mean} [Gy]	≤4.0	0.1 ± 0.2 [0.0;0.5]	2.0 ± 1.9 [0.1;7.2]	-1.9 ± 1.8 [-6.7; -0.1]	<0.001
D _{1cm3} [Gy]	≤30	8.7 ± 12.2 [0.0;30.0]	14.9 ± 14.0 [0.3;44.1]	-5.9 ± 7.1 [-33.2;4.3]	<0.001
Duodenum					
D _{1cm3} [Gy]	≤21	2.4 ± 5.8 [0.0;20.4]	6.6 ± 7.7 [0.3;24.5]	-4.2 ± 6.4 [-23.3;5.4]	<0.001
Stomach					
D _{1cm3} [Gy]	≤21	2.4 ± 5.9 [0.0;20.6]	11.6 ± 7.5 [0.7;28.9]	-8.9 ± 7.1 [-25.3;3.3]	<0.001
Bowel bag					
D _{1cm3} [Gy]	≤21	3.6 ± 7.4 [0.0;24.4]	10.8 ± 12.6 [0.3;54.9]	-6.7 ± 7.5 [-30.5;6.8]	<0.001
Spinal cord					
D _{1cm3} [Gy]	≤18	1.2 ± 3.8 [0.0;13.7]	9.8 ± 5.0 [2.8;20.7]	-1.5 ± 5.1 [-24.0;0.2]	<0.001
Right kidney					
D _{65%} [%]	≤15	0.1 ± 0.1 [0.0;0.2]	0.6 ± 0.6 [0.1;2.1]	-0.6 ± 0.6 [-1.9; -0.1]	<0.001
Left kidney					
D _{30%} [%]	≤15	0.0 ± 0.0 [0.0;0.0]	1.1 ± 2.1 [0.1;7.5]	-1.1 ± 2.1 [-7.4; -0.1]	<0.001

RA = RapidArc, IMPT = intensity modulated proton therapy; D_x = dose received by x% or x cm³ of the volume. D_{mean} = mean dose, V_x = volume receiving less than xGy. HI = homogeneity index (D₅-D₉₅/D_{mean}).

(D_{95%} ≥ 95%); D_x is the minimum dose that covers an x fraction of volume (in % or cm³). The planning objectives for each OAR are reported in Table 1. No explicit optimization constraints were applied to the CHB structure; tolerance thresholds were defined in accordance with²⁰⁻²² and were used for reporting purposes only.

Photon Planning

Volumetric modulated arc therapy in the RapidArc (RA) form was applied to all patients. Plans were designed for a TrueBeam linear accelerator (Varian Medical Systems, Palo Alto, USA) equipped with a Millennium multileaf collimator with a resolution of 5 mm at isocenter using 10 MV flattening filter free photon beams. The optimization was performed with the Eclipse treatment planning system (Varian Medical Systems, Palo Alto, USA) using the Photon Optimizer algorithm (v.15.6)

implemented in the Eclipse planning system. Plans were optimized with 2 partial arcs with a case-by-case setting of the start/stop gantry angles, collimator angle and jaw settings to account for each target specificity. The final dose calculation was performed by means of the Acuros-XB (v.15.6) engine.²³

Proton Planning

Intensity-modulated proton therapy plans were created using pencil beam spot scanning similarly to what described in.¹⁹ The ProBeam proton system (Varian Medical Systems, Palo Alto, USA) was used as a source of beam data. The dose distribution optimization was performed using the fluence-based nonlinear universal Proton Optimizer (NUPO, v15.6)¹⁸ and the Proton Convolution Superposition algorithm (v15.6) was used for the final dose calculation. A constant RBE of 1.1 was applied. Spot spacing was set to 4.25 times the energy-dependent in-air full

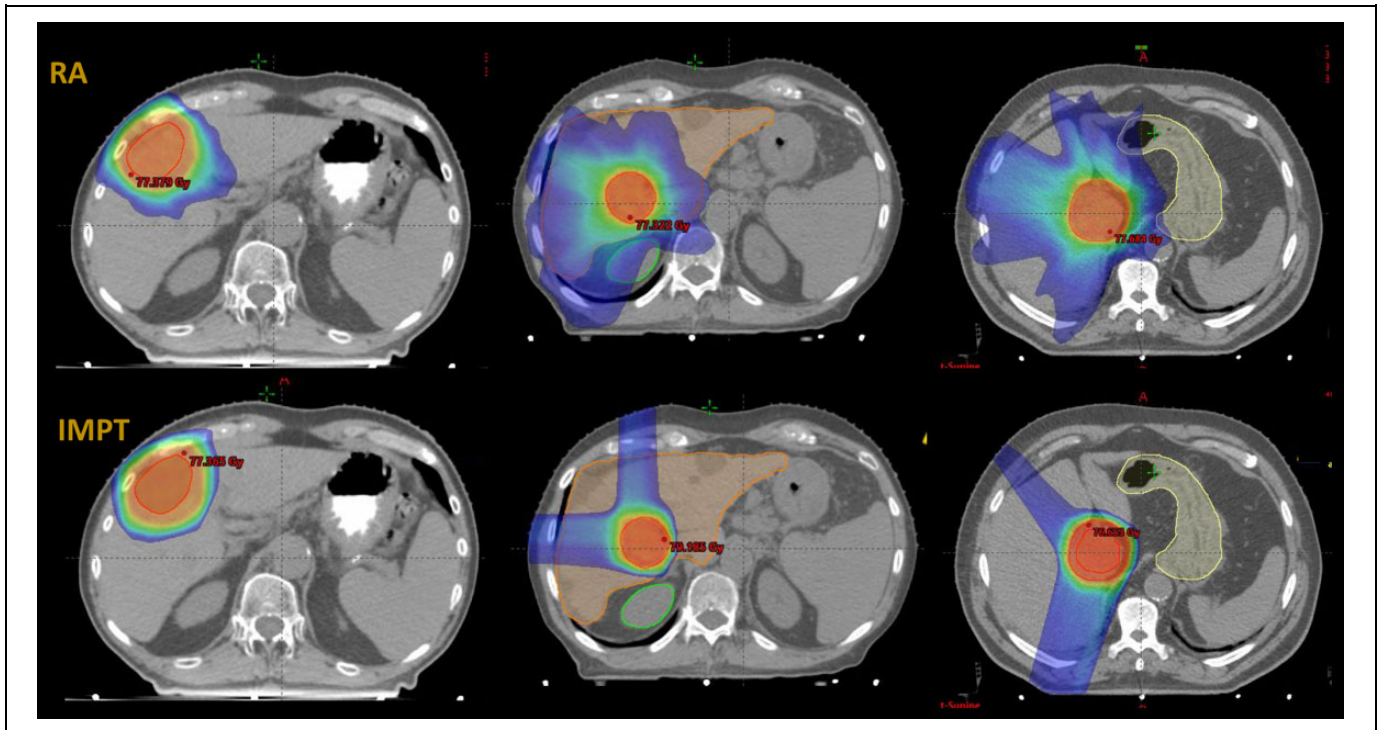


Figure 1. The dose distribution in an axial plane for 3 patients failing in one or more constraints. In the first patient (left column), the constraints on the ribs were violated by both the RA and IMPT plans, the color wash set from 30 to 80 Gy. In the second case (right column) the RA plan violated the stomach maximum dose (color wash from 21 to 80 Gy) while in the third case (central column) RA violated the limits on the healthy liver sparing (color wash from 15 to 80 Gy).

width half maximum spot size at isocenter. To account for “penumbra” effects and improve target coverage, circular axial margins of 3 mm from the PTV were applied both in the proximal and distal directions to enable spot positioning slightly outside the PTV volume. The multi-field simultaneous spot optimization method was selected for all plans. Unlimited optimization was applied, i.e. no restrictions were applied to the dynamic range of intensity modulation or the allowed intensity gradients.

All patients were planned with 2 or 3 beams, the entrance angle of which was tuned according to the target position in the patient. RO, as implemented in the Eclipse system was applied considering ± 3 mm shifts in the isocenter along each axis and $\pm 3\%$ in beam range to the CTV and aimed at minimizing the trade-offs due to the applied uncertainties to the dose-volume constraints in the cost function, as discussed in.¹⁹

Quantitative Assessment of Dose-Volume Metrics

Quantitative metrics were derived from the dose-volume histograms (DVH) and included the mean dose and a variety of V_x and D_x parameters (V_x represents the volume receiving at least an x level of dose in % or Gy). All parameters could be expressed either in absolute (Gy or cm^3) or relative (%) terms. For the CTV, the homogeneity index ($HI = (D_{5\%} - D_{95\%}) / D_{\text{mean}}$) was scored to measure the variance of the dose. The average DVHs were computed, for each structure and each cohort, with

a dose binning resolution of 0.02 Gy. Proton doses are reported in Cobalt equivalent Gy (corrected for the RBE factor).

The Wilcoxon matched-paired signed-rank test was applied to evaluate the significance of the observed differences. The threshold for statistical significance was set at <0.05 .

Results

Figure 1 shows the dose distribution in an axial plane for some patients failing in one or more constraints (showing the plane where the violation is most evident). In the first patient (left column), the constraints on the ribs were violated by both the RA and IMPT plans; the color wash was set from 30 to 80 Gy. In the second case (central column) RA violated the limits on healthy liver sparing (color wash from 15 to 80 Gy) while in the third case (right column) the RA plan violated the stomach maximum dose (color wash from 21 to 80 Gy).

Figure 2 shows the average dose-volume histograms for the CTV, the PTV, and all the OARs included in the study. The detailed numerical summary of the analysis is reported in Table 1. The mean volume of the PTV corresponded to an equivalent sphere with a diameter of 5.0 ± 1.0 cm and a range of 3.3 to 6.8 cm.

Concerning the target volumes, both techniques met on average the coverage constraints for the CTV and the PTV. For the CTV the constraint of $D_{98\%} \geq 98\%$ showed a minor

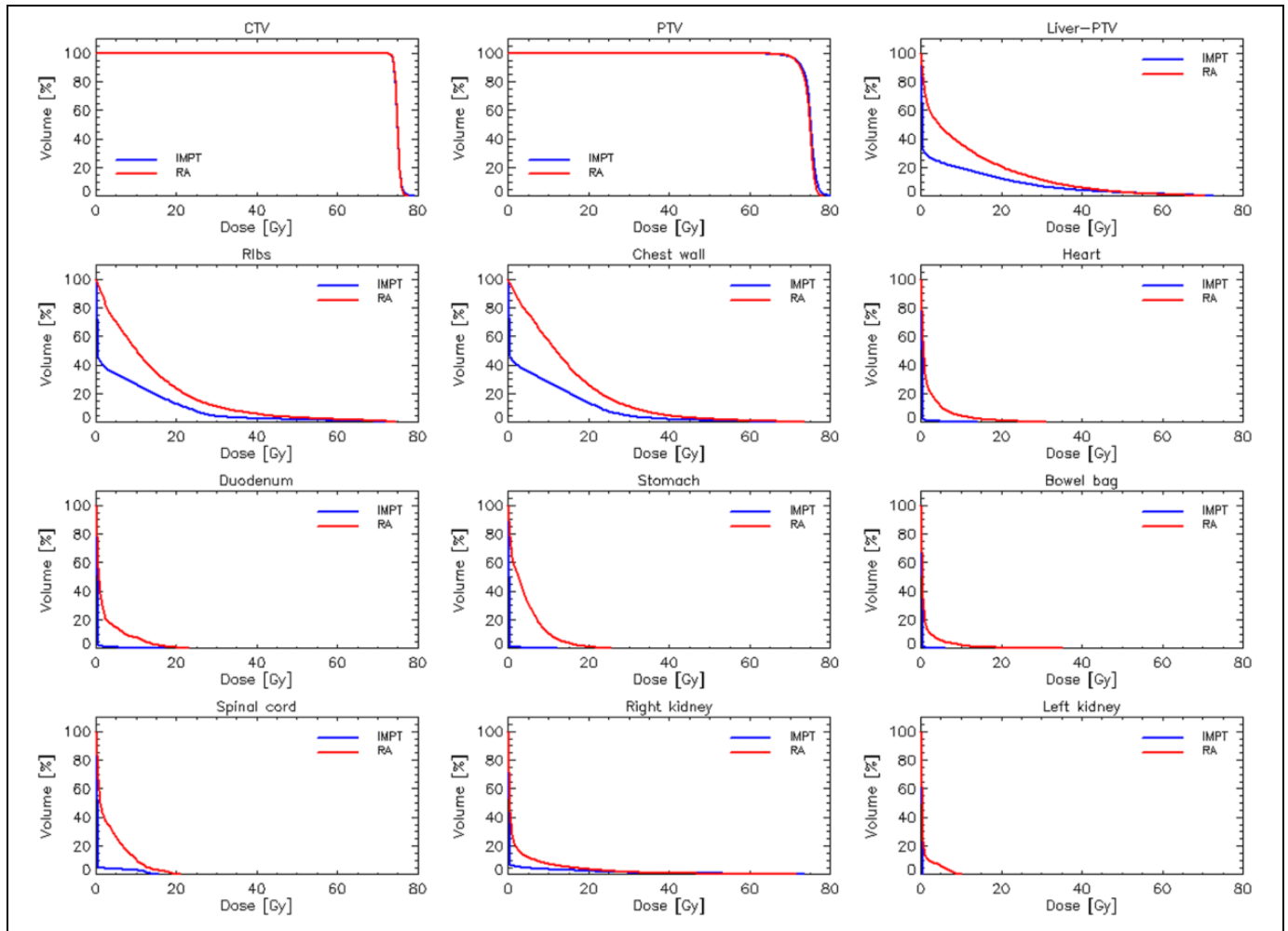


Figure 2. The average dose-volume histograms for the CTV, the PTV and all the OARs accounted in the study.

violation in 5 patients for RA and 10 for IMPT (in all cases with $D_{98\%} \geq 96.5\%$).

The violations of the PTV coverage, which were permitted by the study design, to mitigate the risk of OARs constraints violations, were 11 for RA and 12 for IMPT with a minimum coverage of 90.4% for RA and 89.5% for IMPT.

Concerning the organs at risk and the healthy liver tissue, the IMPT plans showed a systematic and statistically significant improvement compared to the RA technique for all metrics (Table 1).

Both the IMPT and the RA plans respected the dose-volume objectives in all patients only for the spinal cord and the kidneys. In all other structures, the RA plans violated some of the constraints for some of the patients. The detailed summary of the case by case analysis is presented in Table 2.

Concerning the gastro-intestinal structures, RA plans resulted in 2 violations for the duodenum, 3 for the stomach, 4 for the bowel bag. All except one were mitigated by the IMPT technique. The median sparing effect due to the use of IMPT in this subsample of cases, resulted in 10.5, 16.1 and 22.6 Gy for the bowel bag, the duodenum and the stomach, respectively.

Concerning the heart, RA plans resulted in 4 violations for the mean dose and 5 violations for the $D_{1\text{ cm}^3}$ constraint. All were mitigated by the IMPT approach. IMPT resulted in additional sparing of the heart, compared to RA, of 5.6 Gy and 9.5 Gy for the mean and near-to-maximum doses respectively.

The highest number of violations was observed for the ribs (12 for RA) and the chest wall (5 for RA). Only one violation remained for the ribs with the IMPT plans. The improvement resulting from the use of IMPT was of 14.2 and 16.6 Gy for the ribs and the chest wall near-to-maximum doses, respectively.

The volume of non-targeted liver receiving less than 15 Gy did not reach the minimum threshold in 6 cases for RA (none for IMPT) while the mean dose to the healthy liver (liver-PTV) exceeded the limit of 15 Gy in 2 patients for RA. The median gain with IMPT was of 4.9 Gy for the mean liver dose and 155 cm^3 for the volume receiving less than 15 Gy. Concerning the CHB structures, on average both IMPT and RA data respected the clinical thresholds, except for the mean dose to CHB for RA. However, IMPT allowed significant sparing of these structures. In total, with RA, 12 patients exceeded the limits for D_{mean} , $V_{18.5\text{ Gy}}$ and $V_{37\text{ Gy}}$. In comparison, with IMPT the

Table 2. Summary of the Violations of the Protocol Dose-Volume Aims: 43 Cases for the RA Plans Reduced to 2 (in Bold) for the IMPT Plans.

Patient	RA	IMPT	Δ
Ribs $D_{2cm^3} \leq 30$ Gy [Gy]			
P_01	55.0	29.6	-25.4
P_02	40.4	27.6	-12.8
P_03	41.1	27.1	-14.0
P_06	49.4	27.8	-21.6
P_09	59.9	57.8	-2.1
P_16	39.8	27.9	-11.9
P_17	49.1	29.0	-20.1
P_22	56.2	28.6	-27.6
P_24	37.8	25.7	-12.1
P_26	43.5	29.2	-14.3
P_33	43.7	18.6	-25.1
P_34	39.4	25.5	-13.9
Chest wall $D_{30cm^3} \leq 30$ Gy [Gy]			
P_01	46.5	26.8	-19.7
P_09	32.0	29.7	-2.3
P_22	33.9	17.3	-16.6
P_24	34.9	21.3	-13.6
P_33	37.2	13.5	-23.7
Liver-PTV $D_{mean} \leq 15$ Gy [Gy]			
P_10	19.0	7.5	-11.5
P_29	17.8	8.2	-9.6
Liver Volume receiving less than 15 Gy ≥ 700 cm³ [cm³]			
P_01	635	918	283
P_02	569	768	199
P_03	609	987	378
P_09	677	730	53
P_27	608	750	142
P_30	473	705	232
Central hepato biliary structures (CHB) [Gy]			
P_01	21.7	4.1	-17.6
P_02	45.7	34.9	-10.8
P_03	19.5	15.9	-3.6
P_09	38.8	25.9	-12.9
P_10	22.1	9.2	-12.9
P_14	27.6	17.9	-9.7
P_16	24.4	0.9	-23.5
P_21	63.6	60.5	-3.1
P_27	23.8	22.5	-1.3
P_29	53.3	50.8	-2.5
P_30	24.1	13.9	-10.2
P_33	29.4	23.7	-5.7
Heart $D_{mean} \leq 4$ Gy [Gy]			
P_03	6.4	0.1	-6.3
P_12	6.7	1.0	-5.7
P_13	6.3	0.9	-5.4
P_24	5.6	0.4	-5.2
Heart $D_{1cm^3} \leq 30$ Gy [Gy]			
P_03	36.6	3.4	-33.2
P_12	44.1	30.0	-14.1
P_13	38.5	29.0	-9.5
P_15	34.8	29.8	-5.0
P_24	33.2	27.1	-6.1
Bowel bag $D_{1cm^3} \leq 21$ Gy [Gy]			
P_02	32.5	24.3	-8.2
P_14	27.2	11.1	-16.1
P_29	26.3	19.2	-7.1
P_33	31.9	19.2	-12.7
Stomach $D_{1cm^3} \leq 21$ Gy [Gy]			
P_02	28.5	0.3	-28.2
P_29	22.7	0.1	-22.6
P_30	28.9	17.4	-11.5
Duodenum $D_{1cm^3} \leq 21$ Gy [Gy]			
P_30	21.8	0.2	-21.6
P_33	23.5	13.0	-10.5

RA = RapidArc, IMPT = intensity modulated proton therapy; D_x = dose received by x% or xcm³ of the volume. D_{mean} = mean dose, V_x = volume receiving less than xGy.

Table 3. Summary of the Maximum Allowed Dose per Fractions Due to De-Escalation Needs.

Patient	RA	IMPT
P_01	18.75 Gy	25.0 Gy
P_02	15.0 Gy	18.75 Gy
P_03	15.0 Gy	25.0 Gy (18.75)
P_06	15.0 Gy	25.0 Gy
P_09	18.75 Gy (15)	20.63 Gy (18.75)
P_10	18.75 Gy	25.0 Gy
P_12	16.0 Gy	25.0 Gy
P_13	16.0 Gy	25.0 Gy
P_14	16.0 Gy	25.0 Gy (20.63)
P_15	18.75 Gy	25.0 Gy
P_16	20.63 Gy (18.75)	25.0 Gy
P_17	15.0 Gy	25.0 Gy
P_21	25.0 Gy (*)	25.0 Gy (*)
P_22	15.0 Gy	25.0 Gy
P_24	18.75 Gy	25.0 Gy
P_26	16.0 Gy	25.0 Gy
P_27	22.5 Gy (16)	25.0 Gy (18.75)
P_29	18.75 Gy (*)	25.0 Gy (*)
P_30	16.0 Gy	25.0 Gy (22.5)
P_33	16.0 Gy (15)	25.0 Gy (18.75)
P_34	18.75	25.0 Gy

RA = RapidArc, IMPT = intensity modulated proton therapy; (*) CHB structure results largely overlapping with the PTV to be preserved.

number of violations halved to 6 patients; for space reasons in Table 2 only 1 of the 3 toxicity predictors for CHB was reported, the results were consistent for the other two.

In summary, with RA, 20 of the 30 patients (67% of the total)—rising to 21 out of 30 if CHB were included as well—presented one or more violations of the dose-volume constraints. This number dropped to only 2 (7%) in the case of IMPT. Table 3 summarizes the maximum allowed dose per fraction in the risk-adapted de-escalation scheme for each patient in the subgroup; the dose per fraction required to also respect the limits on the CHB is reported in brackets. For 2 patients (#21 and #29), the CHB resulted largely overlapping with the PTV to be protected. With IMPT, it would be possible to prescribe the full dose of 25 Gy in 18/20 cases (90%). These would reduce to 14/21 (67%) if CHB were considered and further down to 12/21 (57%) if the 2 cases with PTV-CHB overlap were excluded. In any case, IMPT plans permitted either maintaining the nominal maximum prescription or a dose higher than that with RA for all patients.

Discussion

The present study investigated the merit of IMPT vs VMAT for the SBRT of HCC in a risk-adapted dose prescription regimen. The findings confirmed the expectations from the earlier study where IMPT was considered for ablative SBRT.⁶ Given the scope of the study and considering the issues regarding motion management and optimization methods discussed below, this study should be considered as a feasibility approach requiring

further refinements to the methods to ensure safe treatment of real patients.

We analyzed a cohort of 30 patients selected as potentially “at-risk” if planned at the highest dose level of 3 fractions of 25 Gy each. It resulted that the photon-based plans violated one or more dose-volume constraints in about 2/3 of these. IMPT potentially allowed to significantly reduce the number of patients requiring a reduced dose prescription. These findings are consistent with the model proposed by Gandhi et al¹⁸ for larger lesions. The central hepatobiliary tract was found to be critical in the treatment of liver lesions with SBRT, and some predictors were identified.²⁰⁻²² In the present study, CHB data were reported although not included in the optimization process since none of the patients included in this study presented cholestasis nor required the implant of any stent after their clinical SBRT treatment with photons.

The slightly inferior target coverage of IMPT was primarily related to the use of RO on the CTV. A side study, was conducted on the “coverage violating patients”; these were re-planned without RO, and the IMPT coverage for CTV respected the planning aims in 6 more cases. Also, a broader lateral and proximal-distal margin would contribute to increasing the coverage at the potential price of a higher near-to-maximum dose to the surrounding OARs. Finally, most of the coverage violations might be mitigated by case-by-case renormalization of the dose distributions to guarantee the requested minimum dose.

Before adopting dose de-escalation, photon VMAT plans should be scrutinized (with appropriate plan comparison)²⁴ for any potential sub-optimality deriving from, e.g. beam geometry. As an example, the 3 cases illustrated in Figure 1 might theoretically be improved by either extended arcs or non-coplanar arc arrangement. This was done for the specific cases included in the study, and the resulting plans were the best achievable by an experienced planning team. Furthermore, the non-coplanar beam arrangement in the abdomen is quite limited by the risk of collisions between the gantry and the couch (and the patient) and would require unusual image guidance procedures, with possibly increased uncertainties in the positioning.

Concerning the primary aim of the study, the OARs, some substantial dose reduction would have been required to fall back within acceptable levels of OARs sparing. The fraction of patients requiring dose de-intensification was reduced to about 7% with IMPT (roughly a factor 10 less than with photons). Some of the violations reported for the photons might be of questionable clinical severity. On the contrary, the possible motion of the gastro-intestinal structures on an inter-fractional basis adds uncertainty on the potential severity of the deviations and should call for a conservative approach. Both considerations point to the need to establish robust and reliable criteria to identify patients suitable for proton therapy. Most of the existing studies suggest the development of algorithms based on normal tissue complication probability models as clearly indicated by several groups.²⁵⁻²⁹ Prayongrat et al³⁰ proposed the use of differential normal tissue complication

probability (Δ NTCP) estimation between photons and protons to assist in treatment selection for HCC patients based on standard clinical predictors like the Child-Pugh status. Although not linearly depending on the dose, the Δ NTCP strongly correlates with it, and the differential improvement shown in our data for all the dose-related metrics would confirm the preferability of IMPT for the challenging patients.

One severe challenge inherent to the treatment of HCC is the motion of the internal organs at risk. This could be due to respiration but also to the time-dependent deformations of the gastro-intestinal tract.

The respiratory induced motion could be mitigated with appropriate 4D delivery with gating. Mizuhata et al³¹ reported about respiratory gating in proton therapy of HCC without the use of fiducial markers for patients with lesions located within 2 cm of the gastro-intestinal tract. They achieved reasonable local control rates without severe toxicity.

Also the possible interplay of motion with the scanning patterns should be considered. Several approaches have been proposed, including rescanning, repainting and beam-specific PTV.³²⁻⁴² Concerning RO, Pfeiler et al⁴¹ investigated a 4D RO method by means of a worst-case scenario (and each scenario was represented by a respiratory phase from the 4D planning CT used in the study, a setup shift and a density perturbation). The authors concluded that RO for pencil beam scanning plans is mainly beneficial for OARs compared to passive scattering protons or non-robustly optimized plans. The results from this study also suggest that multi-field RO for pencil beam scanning protons can be clinically acceptable for most of the patients.

Following the clinical practice with photons, in this study, abdominal compression was applied to all the patients during CT acquisition as a simple mitigator of organs motion. The use of AC with protons is somehow controversial. Lin et al⁴³ concluded that its use enabled a significant reduction in the mean dose to the non-targeted liver and reduced dose degradation within the CTV. Nevertheless, the study found that for patients with small motion, motion mitigation was not needed and produced only a modest overall improvement, while it was deemed necessary for large movements.

Trofimov and Bortfeld⁴⁴ suggested the possibility of limiting the dynamic range of intensity modulation or the allowed intensity gradients to increase the precision and the reliability of the delivery of the modulated plans. Another approach is the single field uniform dose (SFUD) method which can also be applied in combination to beam specific PTVs. Mondlane et al⁴⁵ showed that SFUD, using beam specific PTVs, along with RO methods could bring about a potentially relevant reduction in the probability of normal tissue complication (for the kidneys) in patients with gastric cancer. SFUD was compared to IMPT in some studies for pediatric, prostate and lung cancer cases.⁴⁶⁻⁴⁸ In general, IMPT plans resulted in better target coverage and sparing of the normal tissues and the organs at risk, although at the possible price of a higher trade-off with motion effects.⁴⁸

In the present in-silico study, no rescanning or other methodology was applied. AC, commonly used in clinical practice

with photons, was proposed to mitigate and reduce the impact of respiration on the abdominal structures. For treatment purposes, this might be associated with some gating methodology which is not accounted for in this planning study. Secondly, RO was applied to the CTV, i.e. incorporating the range and isocenter positioning uncertainties which may impact the accuracy and precision of the dose estimation to the target volume. The isocenter shift applied to the RO was set to 3 mm (e.g. Pfeiler et al⁴¹ applied a 2 mm). This approach is not sufficient for structures such as stomach or bowels. In these cases, the only strategy conceptually capable of coping with the inter-fractional variability of the anatomy would be an adaptive on-line re-planning of the cases. There is not yet evidence of this approach in clinical practice with PBT, but it should be considered as an important topic of research for the future.

To conclude the discussion about motion management, we believe that, whatever method or combination of methods would be applied clinically, the daily verification of the efficacy of the methods would be a mandatory step. Appropriate image guidance protocols and/or mechanical tools should guarantee that the dose uniformity degradation induced by the biological motions is actually mitigated by the motion management enforced. This implies that the simpler and the more robust the methods, the easier the task and the better the compliance of the patients and of the system.

An issue in comparative studies between photons and protons is the possible bias in favor of protons because the uncertainties in RBE are usually neglected, as done in the present case with a fixed value of 1.1. A variable RBE with an associated uncertainty (field by field) would be more realistic and might impact on both tumor control and normal tissue complication probabilities. McNamara et al,⁴⁹ reviewing the data and the models for variable RBE, concluded that the notion of fixed RBE is too simplistic and might raise concerns for treatment planning decisions. We acknowledge this as one of the limiting elements of our present study.

Although cost-effectiveness and other economic considerations were not part of the study design, it is important to outline here that, in a finance-limited environment, robust decision making processes should be put in place to select the patients who are expected to benefit most from the (more) expensive proton therapy. Although the dosimetric quality of protons is obviously superior, the incremental benefit for “normal” patients might not justify IMPT. On the contrary, for the challenging cases where severe dosimetric problems might lead to sub-optimal treatments with photons, then IMPT could be fully justified. A model-based approach^{26,27} is therefore envisaged to identify this sub-group of patients and to refer them to the most convenient proton therapy facility.

Conclusion

The results of this in-silico planning study suggest that IMPT might result in advantages compared to photon-based VMAT for HCC patients candidate to ablative SBRT. In particular, the dosimetric characteristics of protons might allow avoiding the need for dose de-escalation in a risk-adapted prescription

regimen for those patients with lesions located in the proximity of dose-limiting healthy structures. Depending on the selection thresholds, the number of patients eligible for treatment at the full dose can be significantly increased with protons.

Authors' Note

Our retrospective in-silico study was approved by notification by the Humanitas cancer center ethics committee. All patients provided written informed consent at time of hospital admission for retrospective use of de-identified data.

Declaration of Conflicting Interests

The author(s) declared the following potential conflicts of interest with respect to the research, authorship, and/or publication of this article: L. Cozzi acts as Scientific Advisor to Varian Medical Systems and is Clinical Research Scientist at Humanitas Cancer Center. All other co-authors declare that they have no conflict interests.

Funding

The author(s) received no financial support for the research, authorship, and/or publication of this article.

ORCID iD

Luca Cozzi  <https://orcid.org/0000-0001-7862-898X>

References

1. Bray F, Ferlay J, Soerjomataram I, Siegel R, Torre L, Jemal A. Global cancer statistics 2018: GLOBOCAN estimates of incidence and mortality worldwide for 36 cancers in 185 countries. *CA Cancer J Clin.* 2018;68:394-424.
2. Dawson L, Normolle D, Balter J, McGinn C, Lawrence T, Ten Haken R. Analysis of radiation induced liver disease using the Lyman NTCP model. *Int J Radiat Oncol Biol Phys.* 2002;53(4):810-821.
3. Kwon JH, Bae SH, Kim JY, et al. Long-term effect of stereotactic body radiation therapy for primary hepatocellular carcinoma ineligible for local ablation therapy or surgical resection. Stereotactic radiotherapy for liver cancer. *BMC Cancer.* 2010;10:475.
4. Culleton S, Jiang H, Haddad CR, et al. Outcomes following definitive stereotactic body radiotherapy for patients with Child-Turcotte-Pugh B or C hepatocellular carcinoma. *Radiother Oncol.* 2014;111(3):412-417.
5. Wang PM, Hsu W, Chung N, et al. Feasibility of stereotactic body radiation therapy with volumetric modulated arc therapy and high intensity photon beams for hepatocellular carcinoma patients. *Radiat Oncol.* 2014;9:18.
6. Scorsetti M, Comito T, Cozzi L, et al. The challenge of inoperable hepatocellular carcinoma (HCC): results of a single institutional experience on stereotactic body radiation therapy (SBRT). *J Cancer Res Clin Oncol.* 2015;141:1301-1309.
7. Durand-Labrunie J, Baumann AS, Ayav A, et al. Curative irradiation treatment of hepatocellular carcinoma: a multicenter phase 2 trial. *Int J Radiat Oncol Biol Phys.* 2020;107(1):116-125.
8. Yoon SM, Kim SY, Lim Y-S, et al. Stereotactic body radiation therapy for small (≤ 5 cm) hepatocellular carcinoma not amenable to curative treatment: results of a single-arm, phase II clinical trial. *Korean J Hepatol.* 2020;26(4):506-515. doi:10.3350/cmh.2020.0038

9. Su TS, Liang P, Liang J, et al. Long-term survival analysis of stereotactic ablative radiotherapy versus liver resection for small hepatocellular carcinoma. *Int J Radiat Oncol Biol Phys.* 2017; 98(3):639-646.
10. Yeung RH, Chapman TR, Bowen SR, Apisarnthanarax S. Proton beam therapy for hepatocellular carcinoma. *Expert Rev Anticancer Ther.* 2017;17(10):911-924.
11. Chuong MD, Kaiser A, Khan F, et al. Consensus report from the Miami liver proton therapy conference. *Front Oncol.* 2019;9:457.
12. Hasan S, Abel S, Verma V, et al. Proton beam therapy versus stereotactic body radiotherapy for hepatocellular carcinoma: practice patterns, outcomes, and the effect of biologically effective dose escalation. *J Gastrointest Oncol.* 2019;10(5):999-1009.
13. Hsu CY, Wang CW, Cheng AL, Kuo SH. Hypofractionated particle beam therapy for hepatocellular carcinoma—a brief review of clinical effectiveness. *World J Gastrointest Oncol.* 2019;11(8):579-588.
14. Chadha AS, Gunther JR, Hsieh CE, et al. Proton beam therapy outcomes for localised unresectable hepatocellular carcinoma. *Radiother Oncol.* 2019;133:54-61.
15. Sanford NN, Pursley J, Noe B, et al. Protons versus photons for unresectable hepatocellular carcinoma: liver decompensation and overall survival. *Int J Radiat Oncol Biol Phys.* 2019;105(1):64-72.
16. Kim T, Park J, Kim B, et al. Does risk-adapted proton beam therapy have a role as a complementary or alternative therapeutic option for hepatocellular carcinoma? *Cancers.* 2019;11(2):230.
17. Mondlane G, Gubanski M, Lind P, Henry T, Ureba A, Siegbahn A. Dosimetric comparison of plans for photon or proton beam based radiosurgery of liver metastases. *Int J Part Ther.* 2016; 3(2):277-284.
18. Gandhi S, Liang X, Ding X, et al. Clinical decision tool for optimal delivery of liver stereotactic body radiation therapy: photons versus protons. *Pract Radiat Oncol.* 2015;5(4):209-218.
19. Cozzi L, Comito T, Fogliata A, et al. Critical appraisal of the potential role of intensity modulated proton therapy in the hypofractionated treatment of advanced hepatocellular carcinoma. *PLoS One.* 2018;13:e0201992.
20. Toesca D, Osmundson E, Eyben R, et al. Central liver toxicity after SBRT: an expanded analysis and predictive nomogram. *Radiother Oncol.* 2017;122(1):130-136.
21. Toesca D, Osmundson E, von Eyben R, Shaffer J, Koong A, Chang DT. Assessment of hepatic function decline after stereotactic body radiation therapy for primary liver cancer. *Pract Radiat Oncol.* 2017;7(3):173-182.
22. Osmundson E, Wu Y, Luxton G, Bazan J, Koong A, Chang D. Predictors of toxicity associated with stereotactic body radiation therapy to the central hepatobiliary tract. *Int J Radiat Oncol Biol Phys.* 2015;91(5):986-994.
23. Vassiliev O, Wareing T, McGhee J, Failla G, Salehpour M, Mourta F. Validation of a new grid based Boltzmann equation solver for dose calculation in radiotherapy with photon beams. *Phys Med Biol.* 2010;55(3):581-598.
24. Stusche M, Kaiser A, Abu-Jawan J, Poettigen C, Levegruen S, Farr J. Re-irradiation of recurrent head and neck carcinomas: comparison of robust intensity modulated proton therapy treatment plans with helical tomotherapy. *Radiat Oncol.* 2013;8:93.
25. Langendijk J, Boersma J, Rasch C, et al. Clinical trial strategies to compare protons with photons. *Semin Radiat Oncol.* 2018;28(2): 79-87.
26. Langendijk J, Lambin P, De Ruyscher D, Widder J, Bos M, Verhaij M. Selection of patients for radiotherapy with protons aiming at reduction of side effects: the model-based approach. *Radiother Oncol.* 2013;107(3):267-273.
27. Rwigema J, Langendijk J, van der Laan P, Lukens J, Swisher-McClure S, Lin A. A model based approach to predict short term toxicity benefits with proton therapy for oropharyngeal cancer. *Int J Radiat Oncol Biol Phys.* 2019;104(3):553-562.
28. Blanchard P, Wong A, Gunn F, et al. Toward a model based patient selection strategy for proton therapy: external validation of photon derived normal tissue complication probability models in a head and neck proton therapy cohort. *Radiother Oncol.* 2016; 121(3):381-386.
29. Cheng Q, Roelofs E, Ramaekers B, et al. Development and evaluation of an on-line three level proton vs photon decision support prototype for head and neck cancer—Comparison of dose, toxicity and cost-effectiveness. *Radiother Oncol.* 2016;118(2): 281-285.
30. Prayongrat A, Kobashi K, Ito Y, et al. The normal tissue complication probability mode-based approach considering uncertainties for the selective use of radiation modality in primary liver cancer patients. *Radiother Oncol.* 2019;135-106.
31. Mizuhata M, Takamatsu S, Shibata S, et al. Respiratory-gated proton beam therapy for hepatocellular carcinoma adjacent to the gastrointestinal tract without fiducial markers. *Cancers.* 2018;10(2):58.
32. Engwall E, Glimelius L, Hynning E. Effectiveness of different rescanning techniques for scanned proton radiotherapy in lung cancer patients. *Phys Med Biol.* 2018;63(9):095006.
33. Zhang Y, Huth I, Wegner M, Weber DC, Lomax AJ. Dosimetric uncertainties as a result of temporal resolution in 4D dose calculations for PBS proton therapy. *Phys Med Biol.* 2019;64(12):125005.
34. Zhang Y, Huth I, Weber DC, Lomax AJ. A statistical comparison of motion mitigation performances and robustness of various pencil beam scanned proton systems for liver tumour treatments. *Radiother Oncol.* 2018;128(1):182-188.
35. Bernatowicz K, Zhang Y, Perrin R, Weber DC, Lomax AJ. Advanced treatment planning using direct 4D optimisation for pencil-beam scanned particle therapy. *Phys Med Biol.* 2017; 62(16):6595-6609.
36. Zhang Y, Huth I, Wegner M, Weber DC, Lomax AJ. An evaluation of rescanning technique for liver tumour treatments using a commercial PBS proton therapy system. *Radiother Oncol.* 2016; 121(2):281-287.
37. Zhang Y, Knopf AC, Weber DC, Lomax AJ. Improving 4D plan quality for PBS-based liver tumour treatments by combining on-line image guided beam gating with rescanning. *Phys Med Biol.* 2015;60(20):8141-8159.
38. Bernatowicz K, Lomax AJ, Knopf A. Comparative study of layered and volumetric rescanning for different scanning speeds of proton beam in liver patients. *Phys Med Biol.* 2013;58(22):7905-7920.
39. Zhang Y, Boye D, Tanner C, Lomax AJ, Knopf A. Respiratory liver motion estimation and its effect on scanned proton beam therapy. *Phys Med Biol.* 2012;57(1):1779-1795.

40. Poulsen P, Eley J, Langner U, Simone C, Langen K. Efficient interplay effect mitigation for proton pencil beam scanning and spot adapted layered repainting evenly spread out over the full breathing cycle. *Int J Radiat Oncol Biol Phys.* 2018;100(1):226-234.
41. Pfeiler T, Ahmad Khalil D, Ayadi M, et al. Motion effects in proton treatments of hepatocellular carcinoma-4D robustly optimised pencil beam scanning plans versus double scattering plans. *Phys Med Biol.* 2018;63(23):235006.
42. Lin L, Kang M, Huang S, Mayer R, Thomas A, Solberg T. Beam-specific planning target volume incorporating 4D CT for pencil beam scanning proton therapy of thoracic tumors. *J Appl Clin Med Phys.* 2015;16(6):5678.
43. Lin L, Souris K, Kang M, et al. Evaluation of motion mitigation using abdominal compression in the clinical implementation of pencil beam scanning proton therapy of liver tumors. *Med Phys.* 2017;44(2):703-712.
44. Trofimov A, Bortfeld T. Optimization of beam parameters and treatment planning for intensity modulated proton therapy. *Tech Canc Res Treat.* 2003;2(5):437-444.
45. Mondlane G, Ureba A, Gubanski M, Lind P, Siegbahn A. Estimation of risk of normal tissue toxicity following gastric cancer radiotherapy with photon or scanned proton beams. *Anticancer Res.* 2018;38(5):2619-2625.
46. Yeung D, McKenzie C, Indelicato D. A dosimetric comparison of intensity modulated proton therapy optimisation techniques for pediatric craniopharyngiomas: a clinical case study. *Pediatr Blood Cancer.* 2014;61(1):89-94.
47. Tang S, Deville C, McDonough J, et al. Effect of intrafraction prostate motion on proton pencil beam scanning delivery: a quantitative assessment. *Int J Radiat Oncol Biol Phys.* 2013;87(2):375-382.
48. Stuschke M, Kaiser A, Poettgen C, Luebcke W, Farr J. Potentials of robust intensity modulated scanning proton plans for locally advanced lung cancer in comparison to intensity modulated photon plans. *Radiother Oncol.* 2012;104(1):45-51.
49. McNamara A, Willers H, Paganetti H. Modelling variable proton relative biological effectiveness for treatment planning. *Br J Radiol.* 2020;93(1107):20190334.